

# High Heat Resistance Can Be Deceiving: Dripping Behavior of Polyamide 4.6 in Fire

Analice Turski Silva Diniz, Julio Marcelo Marti, and Bernhard Schartel\*

Polyamide 4.6 (PA46) is a high-heat-resistant polymer, but it has no dripping resistance under fire. Three commercial grades of PA46 are investigated under UL 94 vertical fire test conditions. Their performances are discussed based on the materials' structural, thermal, and rheological properties. PA46 presents flaming drops, whereas dripping is prevented in the flame-retarded PA46. Friction-modified PA46 has increased flaming dripping. Temperature profiles of the specimens under fire and the temperature of the drops are measured by thermocouples. A UL 94 vertical test configuration consisting of two flame applications is designed to assess the quantitative dripping behavior of the set of materials by the particle finite element method (PFEM). Polymer properties (activation energy and Arrhenius coefficient of decomposition, char yield, density, effective heat of combustion, heat of decomposition, specific heat capacity, and thermal conductivity) in addition to rheological responses in high temperatures are estimated and measured as input parameters for the simulations. The dripping behavior obtained by simulated materials corresponds with the experimental results in terms of time and drop size. A consistent picture of the interplay of the different phenomena controlling dripping under fire appears to deliver a better understanding of the role of different materials' properties.

transition temperatures (glass, melting, and decomposition) to liberate molecules in the pyrolysis process. When decomposition takes place, specific physical and chemical responses can be observed depending on the polymer. Char formation is a benefit when it insulates the polymeric condensed phase, promoting the cessation of burning. The release of non-flammable molecules into the gas phase can promote fuel dilution. However, melt flow and dripping are responses without sure beneficial effects. Mass and heat removal from the pyrolysis zone can help to extinguish the fire but, on the other hand, it can also create a new source of ignition or flame spread within the scenario.

Many works have been dedicated to observing polymers in order to understand their dripping behavior quantitatively and qualitatively.<sup>[1]</sup> The effect of some flame retardants, nanocomposites, reinforcement fillers, and other additives on the dripping phenomena of polymers and polymeric blends were investigated. For various systems, ways were found to

## 1. Introduction

Fire exposure is an extreme condition for polymeric materials. Under fire, thermoplastics are quickly forced beyond their

change the phenomenon (reduction, suppression, transformation of flaming dripping into non-flaming drops, etc.) to fit the needs of certain applications. Such studies revealed the direction in which scientific efforts and industrial developments in flame retardancy should proceed. Above all, this kind of dripping investigation has been helpful to amplify the possibilities of safer end-uses for polymers.


The polymeric materials which had their dripping performance investigated comprehensively in the literature were polypropylene (PP), low-density polyethylene (LDPE), high-impact polystyrene (HIPS), polystyrene (PS), polybutylene terephthalate (PBT), polyamide 6 (Nylon 6 or PA6), polyethylenevinylacetate (EVA), polymethylmethacrylate (PMMA), polycarbonate (PC), acrylonitrile butadiene styrene (ABS), and polyethylene terephthalate (PET).<sup>[2–11]</sup> As listed, the investigations were mainly concentrated on commodities and engineering polymers. Recently, one study on polybutylene succinate (PBS),<sup>[12]</sup> a biodegradable polymer, and two works on bioplastics (poly (lactic acid) – PLA, and polyamide 11 – PA11)<sup>[13,14]</sup> provided insights on the melt viscosity and dripping behavior of materials from other polymer categories.

However, the dripping investigation of a “high-heat-resistant” polymer is somewhat missing. This nomenclature is commonly found in the polymeric markets to designate a class of materials

A. Turski Silva Diniz, B. Schartel  
Federal Institute for Materials Research and Testing (BAM)  
Unter den Eichen 87, 12205 Berlin, Germany  
E-mail: bernhard.schartel@bam.de

J. M. Marti  
International Centre for Numerical Methods in Engineering (CIMNE)  
Technical University of Catalonia (UPC)  
Gran Capitan, s/n, Barcelona 08034, Spain

J. M. Marti  
MECAMAT Group, Department of Engineering, Faculty of Science and Technology  
Universitat de Vic-Universitat Central de Catalunya (UVic-UCC)  
Vic 08500, Spain

 The ORCID identification number(s) for the author(s) of this article can be found under <https://doi.org/10.1002/mame.202300091>

© 2023 The Authors. Macromolecular Materials and Engineering published by Wiley-VCH GmbH. This is an open access article under the terms of the Creative Commons Attribution License, which permits use, distribution and reproduction in any medium, provided the original work is properly cited.

DOI: 10.1002/mame.202300091

with high thermal stability. For semicrystalline thermoplastics, high-heat-resistant equals melting temperatures above 270 °C, as it is reported for polyamide 4.6 (PA46), polytetrafluoroethylene (PTFE), polyether ether ketone (PEEK), and other high-performance polymers.

PA46 has a melting point  $\approx 300$  °C and a service temperature of up to 220 °C without loss of its intrinsically elevated mechanical properties. PA46 outperforms related materials such as polyamide 6, polyamide 6.6, and polyphthalamide (PPA) in this respect. PA46 meets requirements for very specific applications in the E&E and automotive markets, often to replace metal, where the material needs to withstand high temperatures and stresses. Some examples are electronic connectors, gears, outdoor power equipment, engine valve timing systems, etc.<sup>[15]</sup> A V-classification in UL 94 fire testing is a common requirement.

The UL 94 vertical test has been the most common method used to assess dripping during the fire. It became established as the easiest method because the reaction to a small flame is observed, allowing observation of whether or not dripping occurs. Dripping is a critical factor, as different ratings can be given depending on whether it consists of flaming or non-flaming drops.<sup>[16]</sup>

Aiming to provide comprehensive data on high-heat-resistant polymeric dripping, this work presents the performance of PA46 materials under UL 94 conditions. The UL 94 test is suitable to evaluate the heat resistance of polymers, as it simulates exposure to a high heating rate. Temperature profiles of the specimens during the test were monitored by thermocouples to identify possible heat barrier/resistance effects during the fire. The transition temperatures of the materials were assessed, and curves of thermal decomposition and viscosities from materials and their respective collected drops were analyzed. Key properties were measured to be used as input in a model using the particle finite element method PFEM<sup>[17]</sup> as a quantitative tool. Experimental dripping was discussed and compared to the simulated dripping descriptions.

## 2. Experimental Section

### 2.1. Materials

The evaluated materials were commercially available by DSM. Investigated types of polyamide 4.6 material were a polyamide 4.6 (Stanyl TE300), a polyamide 4.6 combined with a flame retardant (Stanyl TE351), and a polyamide 4.6 wear- and friction-modified by addition of polytetrafluoroethylene (Stanyl TW371). These materials will be referenced hereafter as PA46, PA46/FR, and PA46/PTFE, respectively. The PA46/FR contains a concentration < 10 wt.% of aromatic bromine compounds (without brominated diphenyl ethers and biphenyls) in combination with antimony compounds. The PA46/PTFE contains a portion of  $\approx 13$  wt.% polytetrafluoroethylene. All materials were kindly provided by TER HELL Plastic GmbH (Herten, Germany).

### 2.2. Methods

The materials' reaction to a small flame was assessed by UL 94 vertical flammability test (Underwriters Laboratories Inc.).<sup>[16]</sup>

The specimens for this test were prepared by injection molding according to the manufacturer's recommendations, in dimensions of  $125 \times 13 \times 3$  mm<sup>3</sup>. The specimens were weighed before and after testing. Drops generated were collected as described in,<sup>[12]</sup> weighed, and identified according to their sources (first or second ignition) for further investigations as follows. Drops originating during the first flame application and/or in the first after-flame time were identified as dFIG. Drops originating during the second flame application and/or in the second after-flame time were named dSIG.

During the UL 94 V test, burning specimens were recorded using a model Therma CAM S65 FLR infrared camera and a conventional digital camera. The infrared (IR) videos were taken using a temperature range of the camera of 350 to 1500 °C, with emissivity set to 0.91.

The temperature distribution in the polymer during burning was assessed by 5 thermocouples (type K, NiCr/NiAl, detection range 0–1100 °C) coupled inside the specimen, as detailed below. The same type of thermocouple was used to measure the temperature of the melting drops released at 8 cm below the specimen end tip.

Thermal investigation of the materials included thermogravimetric analysis (TGA) and differential scanning calorimetry (DSC). TGA was performed under a nitrogen atmosphere, from 25 to 900 °C at a heating rate of 10 °C min<sup>-1</sup>. Fine powder samples of  $10.0 \pm 0.1$  mg weight were analyzed using a NETZSCH TG 209F1 instrument. DSC analysis was carried out in a NETZSCH DSC 204F1 Phoenix instrument, using pellet samples of  $8.0 \pm 0.1$  mg, at a heating rate of 10 °C min<sup>-1</sup> under nitrogen atmosphere.

Rheological properties were investigated using the MCR 501 Anton Paar plate-plate rheometer. Samples were previously stored for 48 h at 23 °C and 50% relative humidity. The first measurements were taken in oscillation mode at 300 °C, with an angular frequency between 100 and 0.1 rads<sup>-1</sup> and a deformation amplitude of 0.5%. In addition, measurements were carried out in the range from 300 to 40 °C at 0.1 rads<sup>-1</sup> with 0.5% deformation.

#### 2.2.1. Numerical Procedure

The dripping behavior was numerically investigated by particle finite element method (PFEM),<sup>[17]</sup> a numerical tool developed at International Centre for Numerical Methods in Engineering (CIMNE, Spain) to combine the robustness of mesh-based techniques with the advantages of particle-based methods. Following a Lagrangian description, the mesh nodes behave like particles moving according to the equations of motion and transporting their momentum together with all their physical properties.<sup>[18]</sup> Whereas for multifluid analysis the surface tensions were needed for describing the interface sufficiently, PFEM easily define any free-surface position, and thus it is particularly useful for fluids for which a large deformation of the physical domain was observed. PFEM solves a variety of fluid-structure problems, being suitable for the melt flow and dripping study.<sup>[19]</sup> PFEM was already applied to model satisfactorily the dripping behavior of cables made from thermoplastic polyurethane (TPU) under fire.<sup>[20]</sup> The dripping simulation of a typical non-charring polymer

(polypropylene) was also made using PFEM through exposure to different heat fluxes<sup>[19]</sup> and under UL 94 conditions<sup>[21,22]</sup> limited to one flame application. The dripping of an engineering polymer system (polycarbonate/acrylonitrile-butadiene-styrene)<sup>[9]</sup> in the UL 94 scenario using one flame application was assessed by PFEM, too. In the present work, PFEM deals with some materials (PA46) that may offer more resistance to melt flow than those studied before. The assessment of the dripping performance of these “high-heat-resistant” materials by PFEM addresses high-performance end-uses. A two-flame application test configuration was applied to depict better the UL 94 vertical test by the acquirement of information from different dripping occasions. The details of the modeled problem are described below.

In the PFEM, the initial viscosity at room temperature was set to  $10^6$  Pa.s to guarantee a solid state. For temperatures above 400 °C, the viscosity was set to follow the same tendency found for 400 °C in the measurements. Additionally, other overall properties were required as input to perform the numerical investigation: the activation energy and Arrhenius coefficient of decomposition, char yield, density, effective heat of combustion, heat of decomposition, specific heat capacity, and thermal conductivity. Once PFEM considers each calculation particle as a single point of properties, no individual properties of additives were measured, but overall material properties. For this, additional TGA measurements with 2, 5, 10, and 20 °C min<sup>-1</sup> were conducted under nitrogen atmosphere, enabling the kinetic analysis of decomposition. The activation energy and Arrhenius coefficient were evaluated from a first-order Arrhenius equation.<sup>[23]</sup> Char yield values for PA46 and PA46/FR were obtained from thermogravimetry at a temperature of 500 °C, and for PA46/PTFE at 650 °C right after the main decomposition step. Density was obtained from the samples’ geometry and mass. The apparent effective heat of combustion (EHC) was obtained from forced-flaming behavior monitored in the cone calorimeter (FTT equipment) under a heat flux of 50 kW m<sup>-2</sup>. Although, the works on PA46 are rather rare, the thermal decomposition of aliphatic polyamides was intensively studied and reviewed several times.<sup>[24,25]</sup> A series of volatile pyrolysis products – hydrocarbons, nitrogen-containing species, and low molecular gases CO<sub>2</sub>, CO, H<sub>2</sub>O, NH<sub>3</sub>, and HCN have been identified, as well as monomers, linear oligomers, and characteristic cyclic products for poly lactams and diamino-diacid based polyamides. Whereas the thermal decomposition starts from homolytic scission of the N-alkylamide or peptide C(O) NH bonds, the subsequent pathway, and products depend strongly on experimental conditions, for instance, the additives incorporated. Determining the char yield, the decomposition kinetics, and the apparent EHC, all the important differences in decomposition in terms of fuel amount, fuel release rate, and quality of fuel was covered sufficiently.

The heat of decomposition was estimated to be that found for polyamide 6,6 at<sup>[26]</sup> and set to the same value for all simulated materials. The specific heat capacity of PA46 at 100 °C was determined via DSC in accordance with the ISO 11357-4 standard and was also estimated to be the same value for all materials. Thermal conductivity was measured using the transient plane heat source method with a TPS 1500 Hot Disk instrument, in accordance with ISO 22 007. The input parameters for modeling are reported in Table 1.

**Table 1.** Input parameters for PFEM simulation.

Parameter	PA46	PA46/FR	PA46/PTFE	Units
Activation energy (Ea)	228.02	166.24	207.63	kJ mol <sup>-1</sup>
Arrhenius coefficient (A)	$6.2 \times 10^{14}$	$8.5 \times 10^{10}$	$1.3 \times 10^{13}$	s <sup>-1</sup>
Char yield (CY)	3	15	1	%
Density ( $\rho$ )	1161	1374	1247	kg m <sup>-3</sup>
Effective heat of combustion (EHC)	26.3	12.6	22.7	MJ kg <sup>-1</sup>
Heat of decomposition (Hdec)	1 390 000	1 390 000	1 390 000	J kg <sup>-1</sup>
Specific heat capacity (c)	2092	2092	2092	J kg <sup>-1</sup> K <sup>-1</sup>
Thermal conductivity (k)	0.351	0.295	0.346	Wm <sup>-1</sup> K <sup>-1</sup>

A fourth part of the original specimen was created for the PFEM simulations ( $125.0 \times 6.5 \times 1.5$  mm<sup>3</sup>) using the GiD developer version 15.1.6d. The 3D geometry consisted of 3285 nodes and 12 095 tetrahedral elements. Boundary conditions conform with those presented in.<sup>[20]</sup> The model set-up included 4 phases: the first flame application, the first after-flame time, the second flame application, and the second after-flame time. Each phase lasted 10 s. During flame applications, the discretized specimen was exposed to an external heat flux. A maximum heat intake of 150kWm<sup>-2</sup>.<sup>[27]</sup> was applied to the bottom of the specimen. The heat flux distribution through the specimen bar was calculated by the equation described in.<sup>[9]</sup> Heat feedback from the flame and polymer combustion were considered. The effective heat of combustion multiplied by mass loss rate represented this additional heat in the model calculations.

Current models prevailed to simulate the burning behavior of polymeric materials are rather sufficient,<sup>[28,29]</sup> so that the proper determination of the input parameters has increasingly become key for significative simulations. Thus, the proper determination and approximation of the input parameters done (Table 1) were the fundament to get a meaningful insight. What was more, the difference in char yield, in the apparent effective heat of combustion, and in the viscosity versus temperature (discussed later in the result and discussion part) were the most important input parameters enabling to simulate of the impact of charring, flame inhibition and dripping on the burning behavior in UL 94 tests.

## 3. Results and Discussion

### 3.1. Transition Temperatures

Polyamides can present different characteristics depending on the number of amide links per given chain length. One that is of great interest for the study of dripping is the melting temperature (T<sub>m</sub>). PA46 is an aliphatic polyamide with an elevated T<sub>m</sub> produced by the polycondensation of 1,4 diamino-butane and adipic acid. Its chemical form and properties are compared to other classic polyamides in Figure S1 in the Supporting Information. The melting temperature of PA46 is increased (295 °C) by its higher molecular weight. In PA46 the chemical links are distributed with greater symmetry along the macromolecules, favoring the crystal packaging, so that PA46 has superior crystallinity

and faster crystallization. As the polar amid groups (CONH) are placed at very short distances from each other in the main chain, there is a high degree of H-bonding between macromolecules, resulting in strong mechanical and thermal properties as well as higher water absorption.<sup>[15,30–32]</sup>

Results from DSC measurements revealed the transition temperatures of the set of materials studied here. DSC curves are given in Figure S2 in the Supporting Information.

The three investigated materials presented curves with almost indistinguishable steps of glass transition temperature ( $T_g$ ) around 70 °C. The reason is the nature of those highly crystalline materials, which had only a small amorphous portion available to undergo glass transition. The flame-retarded version and the blend demonstrated a slight decrease in  $T_g$  as compared to the PA46. Additives increase the free volume between polymer chains, which can facilitate the sliding of molecules at lower temperatures, thus reducing  $T_g$ .

There is no significative difference between the melting temperature ( $T_m$ ) of the PA46 (292 °C) and the flame-retarded PA46 materials (290 °C). The blend PA46/PTFE presented two endothermic events, one for each polymer content: an earlier PA46 melting peak was observed at 286 °C (70.4 J g<sup>-1</sup>), followed by a melting peak of polytetrafluorethylene at 325 °C (6.6 J g<sup>-1</sup>).

### 3.2. Burning And Dripping Behavior

Figure 1 shows the specimen tips after the UL 94 vertical test and their drops released. PA46 achieved the V-1, PA46/FR the V-0, and PA46/PTFE the V-2 classification for 3-mm thick specimens. These results are in good accordance with the ratings found in the data sheets for specimens of 1.5-mm thickness, where PA46 is V-2, PA46/FR is V-0, and PA46/PTFE is HB. Only the PA46 and PA46/PTFE produced drops during the flammability test. For those, the original specimen dimensions (125 × 13 × 3 mm) changed after the test, as observed from the average measurements of cooled specimens at room temperature after testing. Due to deformation, the specimen height increased to 128 mm ± 2.0 (PA46) and 133 mm ± 5.0 (PA46/PTFE). Moreover, the maximum expansion in the specimen tip after test was 14 mm ± 1.0 in width × 4 mm ± 1.0 in thickness for PA46, while PA46/PTFE had 16 mm ± 1.0 in width × 7 mm ± 1.0 in thickness (see Figure 1a and Figure 1c).

The PA46/FR specimen maintained its original dimensions after testing (Figure 1b), with almost imperceptible superficial burning damage. Table 2 shows the average total mass loss for each material.

For PA46, flaming droplets left the bar, contributing to the specimen's extinguishment. The total after-flame time of the test was about 40s. The number of drops generated in the First Ignition phase varied between zero to one, and in the Second Ignition between one to three. All drops collected from the First Ignition (dFIG) were obtained after flame application (above 10s), while all drops collected from the Second Ignition (dSIG) were generated during the flame application (under 10s). When drops from PA46 reached the cotton, it was ignited. The same drops stopped burning within 2s when they reached the aluminum foil beneath the specimen destined for collecting drops. It is important to con-

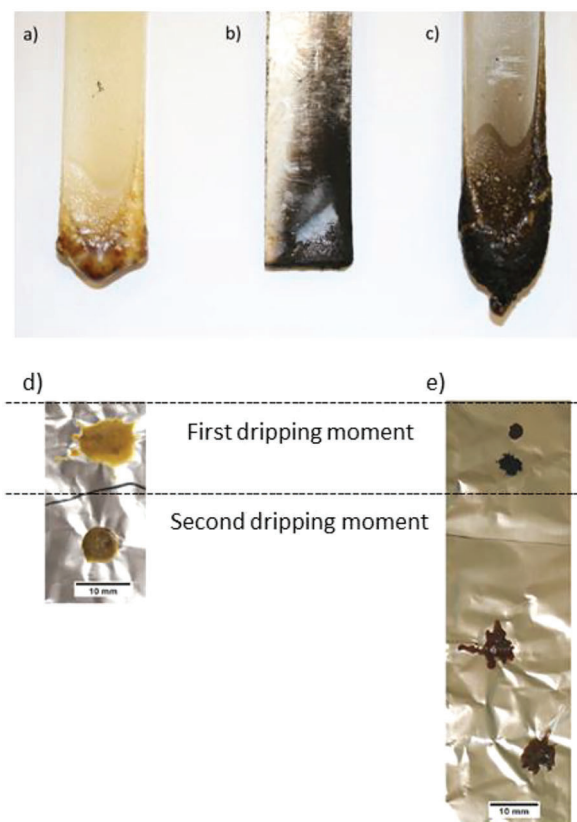


**Figure 1.** Specimen tips of a) PA46, b) PA46/FR, and c) PA46/PTFE after test, and the drops released from d) PA46 and e) PA46/PTFE.

**Table 2.** Mass losses based on specimen and drop weights.

Specimen	Total mass loss [wt.-%]	Mass loss by dripping [wt.-%]	Mass loss by volatilization [wt.-%]
PA46	1.8	1.4	0.4
PA46/FR	0.9	-	0.9
PA46/PTFE	7.8	7.5	0.3

sider that the weight of the collected drops might differ from that portion of mass lost in the moment of detachment due to mass loss by flaming.

Over the tests, it was noticed that all dFIG from PA46 were thinner and more brittle than the dSIG ones (Figure 1d). Their shape was characterized by a high dispersion on the aluminum foil, indicative of a possible low viscosity of the melted material released during First Ignition. On the other hand, dSIG were apparently heavier than dFIG, with a well-delimited, round shape.

PA46/FR released pronounced black smoke during test. A typical increase of this characteristic in aliphatic nylons caused by halogenated fire retardants was reported.<sup>[33]</sup> The soot can be seen to remain on the specimen (Figure 1b). For this nondripping material, the volatilized portion corresponds to the total mass loss, which was the lowest of the three materials.

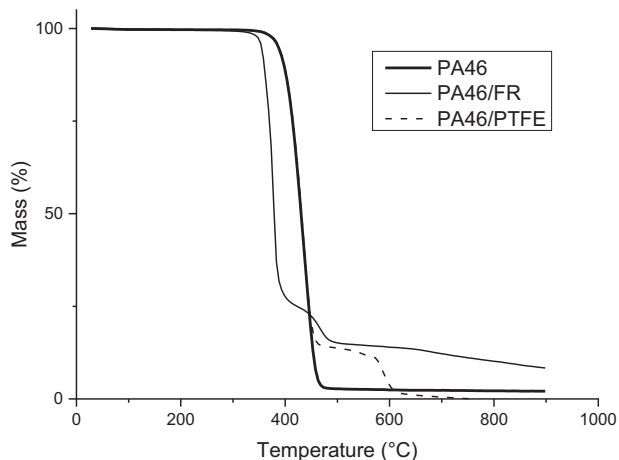


**Figure 2.** Thermogravimetric curves of original materials.

The specimens of friction-modified PA46 (PA46/PTFE) presented bubbling and sparking during burning. The addition of PTFE does not prevent or limit the dripping phenomena, as described in other works on specific anti-dripping PTFE fibers.<sup>[9,34]</sup> Between 1 and 2 flaming drops left the specimen during the First Ignition and 3 – 16 during the Second Ignition. Due to this high variability, the total after-flame time varied from 40 to 80 s. Collected drops had pronounced differences in size, observable on the collecting aluminum foils (Figure 1e). The dFIG had small diameters, while dSIG had larger formats caused by a larger spread. All dFIG were obtained after application (above 10s), while dSIG were generated during the flame application (under 10s). The drops readily ignited the cotton, while on the aluminum foil they kept burning for 2 – 7 s until extinguishment. Thus, these drops had a black appearance and were very lightweight. Accordingly, the dripping masses tend to be higher at the moment of fall than when they are weighed after extinguishment. The portion of dripping and volatilized masses for both dripping materials were approximated in Table 2. The dripping losses were the main mechanism of mass loss. The sort of dripping obtained for PA46 and PA46/PTFE was the small-sized type, according to the classification designed in,<sup>[3]</sup> defined by random-chain scission as the main mechanism of decomposition of polyamides. The addition of PTFE, which is

a polymer with depolymerization as its main decomposition mechanism,<sup>[31,35]</sup> did not alter the blend's type of dripping.

### 3.3. Decomposition

Thermogravimetric results are plotted in **Figure 2** and detailed in **Table 3**. PA46 decomposes between  $\approx 400$  and  $460$  °C. After that, 1.0 wt.% is slowly lost between 460 and  $900$  °C, with a portion of  $2.0\% \pm 0.1$  remaining as residue at  $900$  °C. In PA46/FR the thermal decomposition of PA46 was anticipated to the drastically narrow range of  $\approx 370$  and  $380$  °C. This reduced thermal stability is attributed to some condensed-phase activity, as halogenated additives and metal synergists tend to initiate or catalyze degradation in aliphatic nylons by hydrogen halides.<sup>[33]</sup> A second step of decomposition between  $450$  and  $485$  °C expressed the flame-retardant mass loss ( $\approx 10$  wt.%). After that, a continuous mass loss of 6.5 wt.% was observed until  $900$  °C, when a residue of  $8.0\% \pm 0.5$  remained.

PA46/PTFE exhibited no alteration in the onset and endset temperatures for the main decomposition step of PA46. The second step observed in the blend curve corresponds to the decomposition of 13 wt.% of PTFE content between  $570$  and  $606$  °C. After that temperature, a small mass loss takes place until no residue is left at  $750$  °C. The amount of PTFE friction modifier found in this modified material may also explain the presence of dripping phenomena. The action of PTFE anti-dripping types is caused by a physical effect of microfibrils formed during processing which shrink back under fire, preventing dripping release.<sup>[33]</sup> PTFE anti-dripping types are usually added at very low levels ( $\leq 0.9\%$ ) to a polymeric matrix or blend.<sup>[9,34–36]</sup>

As to the drop's thermal decomposition (**Figure 3**), a previous step in the TG curves indicated some release of low-molecular-weight pyrolysis products (see Table 3). The thermal stability of PA46 drops (dFIG and dSIG) was essentially preserved (Figure 3a), with a slight increase in the residue portion of both as compared to PA46. In PA46/PTFE drops, PA46 started to decompose around  $390$  °C, earlier than PA46. The content of PA46 in PA46/PTFE drops was higher in dSIG than that observed in dFIG. The portion of PTFE inside dFIG increased (14.6%, starting at  $540$  °C), while dSIG decreased to almost half (6.8%, starting at  $570$  °C), clearly shown in Figure 3b by the near disappearance of this step in TG curve and corresponding peak

**Table 3.** Thermal decomposition data.

SAMPLE	Previous step [wt.-%]	1st Decomposition step				2nd Decomposition step				Residue at 900 °C [wt.-%]
		T onset	T endset	Mass loss	T max	T onset	T endset	Mass loss	T max	
Drops		[°C]	[°C]	[wt.-%]	[°C]	[°C]	[°C]	[wt.-%]	[°C]	
PA46	–	402	458	97.0	436	–	–	–	–	2.0
dFIG	2.7	407	452	92.0	434	–	–	–	–	3.5
dSIG	2.9	400	449	93.4	425	–	–	–	–	2.9
PA46/FR	–	371	380	75.2	378	428	481	9.8	498	8.3
PA46/PTFE	–	403	451	86.0	435	572	606	13.0	590	0.0
dFIG	1.9	391	441	75.6	421	540	593	14.6	564	6.6
dSIG	2.1	395	449	84.8	406	570	598	6.8	586	4.7

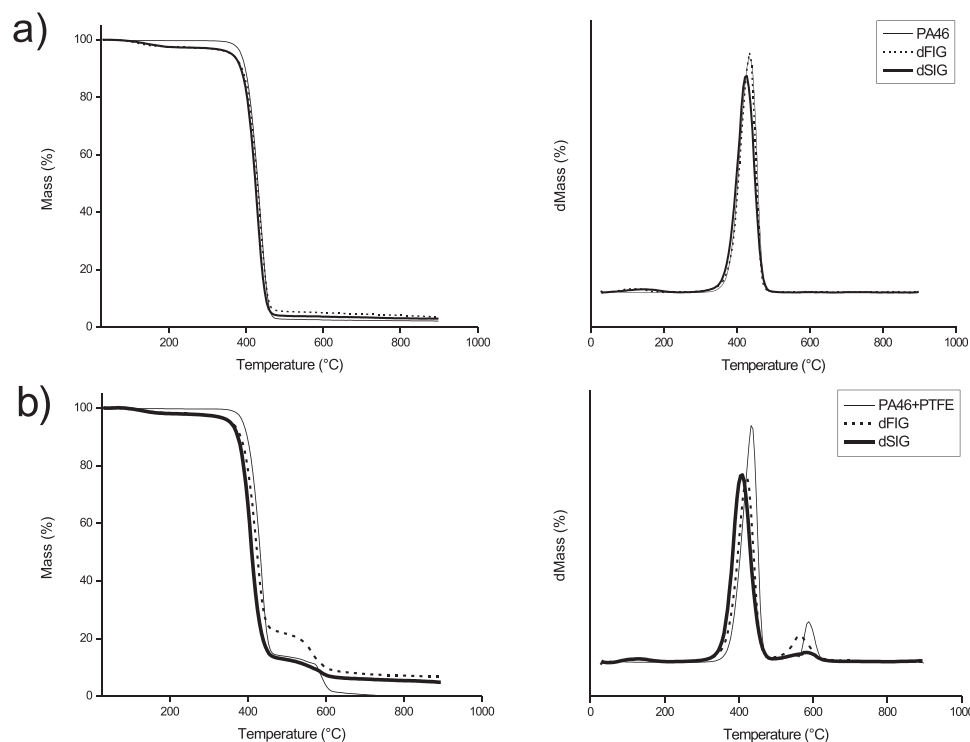


**Figure 3.** Thermogravimetric curves of the drops.

at DTG. The residue increment in the drops of PA46/PTFE was significant (Table 3).

### 3.4. Dripping Temperature

Below the UL 94 V test set-up, thermocouples caught the temperature of drops generated in first and second ignitions (TdFIG and TdSIG). First, the falling drops met the aluminum foil after 8 cm of fall. Then, only after their natural extinguishment, the temperature measurement was proceeded. The TdFIG registered for PA46 was  $88 \pm 33$  °C, and for PA46/PTFE it was  $238 \pm 36$  °C. This indicates that the formation of dripping for each of these materials started from different temperatures, or that some polymer dripping released more heat in the process of burning and falling than the other, or both. The same happens for TdSIG, where PA46 had  $130 \pm 79$  °C and PA46/PTFE had  $316 \pm 18$  °C.

### 3.5. Specimen Temperature

The temperature distribution inside the tested specimens was measured by thermocouples at 5 different points. This setup and the temperature profiles acquired after first and second ignitions are displayed in **Figure 4**.

At the first moment, roughly the same profile of heat distribution was observed for PA46 and PA46/FR. They achieved temperatures above  $T_g$  from T1 to T4. In comparison, the heat spreading in the blend specimen was much shorter, limited only to points T1 and T2.

The point T1 provided an approximation of pyrolysis temperature during the test; for dripping materials, this was considered the dripping temperature.

The point T1 after the first flame application in PA46 and PA46/FR achieved 401 °C and 382 °C, respectively. These values are close to their respective decomposition temperatures ( $T_d$ ). At the same point, PA46/PTFE registered 290 °C, which is close to PA46 melting temperature ( $T_m$ ). In this aspect, the dripping materials (pure polymer and modified polymer) differ from each other on the temperature of drip release. PTFE is a polymer with higher heat resistance than PA46, with working temperatures of up to 260 °C.<sup>[37]</sup> This addition may improve the heat resistance of the blend in the solid state as promised by the suppliers; however, in the melt state, the dripping resistance of the blend was clearly lower than that of the neat polymer. Moreover, both dripping materials produced flaming drops, which indicates that they both achieved ignition temperatures.

The explanation is found in the char formation. The specimen tip of PA46/PTFE was covered with much more char than that observed for PA46. This physical barrier keeps the temperature inside the blend specimen low, as verified by the measurement. In the thin surface exposed to fire, however, where the thermal decomposition of the polymeric constituents is initiated and cross-linking starts, leading to char, the temperature was surely higher than that measured inside. Here dripping was released from the surface during char formation, as a highly degraded material. The TGA results found for PA46/PTFE drops (dFIG and dSIG) correspond with this, presenting increased portions of residue and reduced thermal stability.

After the second flame application, the temperatures for the specimen tips (T1) were: 361°C (PA46), 273°C (PA46/FR), and

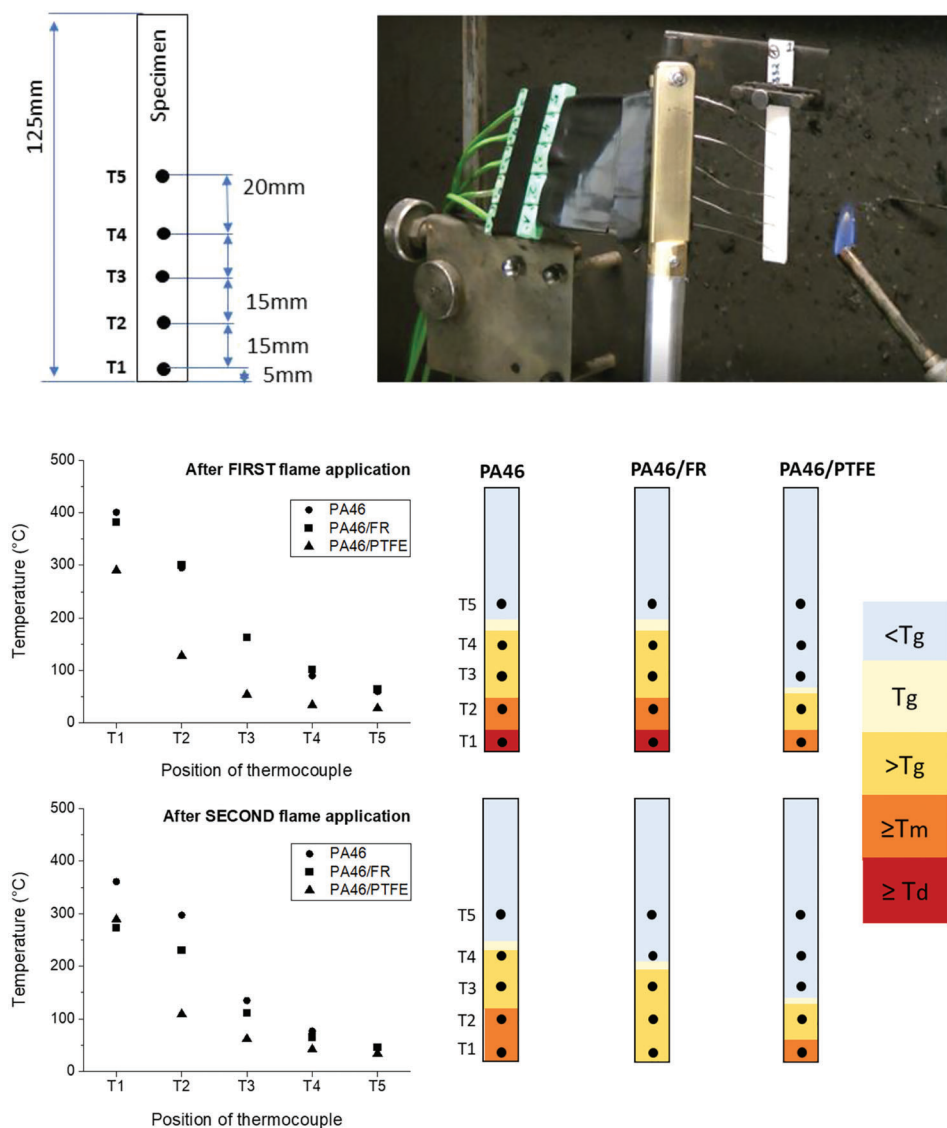


**Figure 4.** Set-up of specimen temperature measurements and results.

289°C (PA46/PTFE). This amounts to a reduction of 40°C for PA46 and 109°C for PA46/FR as compared to the results of the moment after the first flame application. PA46/PTFE had nearly the same  $T_m$  temperature as before. Cooling effects by dripping, flame-retardant action, and char formation are behind this behavior, respectively.

The graphs in Figure 4 detail the temperature values at points T1 to T5 inside the specimen. During the first flame application, PA46 and PA46/FR practically overlap. The FR does not act instantaneously as a cooling agent for the polymeric specimen during the test, as usually occurs for FR of dripping action, such as melamine cyanurate,<sup>[12]</sup> which had a reduction of temperature in the specimen tip, compared to the neat polymeric specimen. Instead, the halogenated flame retardant started its action in the gas phase only once the range of temperature decomposition of the polymer was achieved. Then, according to the evaluation of the profile, the flame retardant is activated, i.e., starts debromi-

nation, after the first moment of measurement, and the effect of flame inhibition is observed after the second flame application, when the temperature of the specimen is decreased.

Of the three investigated materials, the blend had the lowest temperatures measured at the points during the first and second flame applications. Additionally, PA46/PTFE exhibited no significant change in the pattern of temperature distribution between the two moments measured. The protective effect of char was repeated in the second moment measured, preventing heat from spreading easily along the specimen throughout the condensed phase.

In Figure 5, infrared images taken during UL 94 v tests are presented. These thermal images were used only for general evaluation purposes and comparison with the temperatures measured by the thermocouples. The colors registered by the IR camera approximate the observed temperatures in the specimen as follows: blue color as room temperature (23 °C), pink color

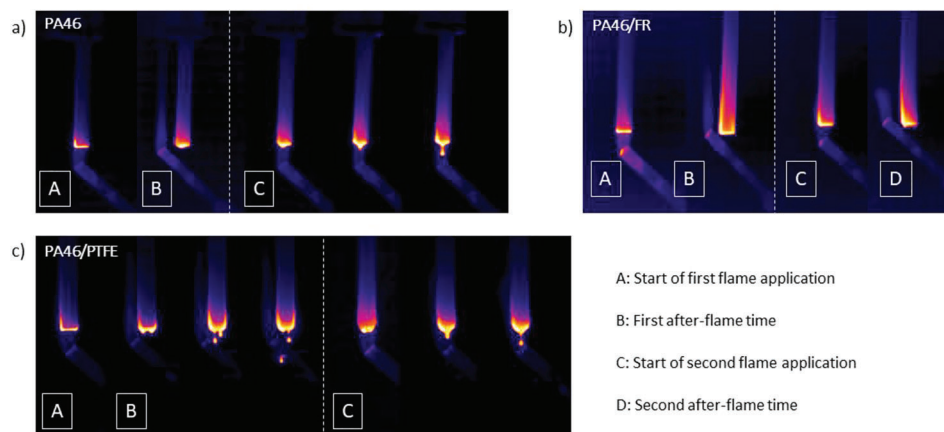


**Figure 5.** IR-camera images of specimens' temperature during the test.

as heat conduction ( $\approx 200$  °C and 300 °C), and yellow color as burning front (above 300 °C to 600 °C). Thus, the region of maximum heat is depicted by a thin yellow region at the bottom end of the specimens, known as the pyrolysis zone.

For PA46, this yellow region observable during the first flame application (Figure 5a,A) was enhanced after the removal of the burner (Figure 5a,B). In the second flame application (Figure 5a,C) this yellow region generated a neck below where dripping started, while some heat dissipated along the specimen. Drops were released following the model of side-edge flux to form one detachment point.

Compared to PA46 and PA46/PTFE (Figure 5a,c), PA46/FR (Figure 5b) exhibited higher heat conduction along the specimen during both flame applications (A and C) and in the after-flame times (B and D). The spread of heat occurs while no dripping or dimensional deformation in the bar is shown. Once the thermal conductivity of PA46/FR was found to have the lowest value (Table 1), the role of dripping on specimen cooling under test was clearly highlighted.

For PA46/PTFE, the thin yellow area at first ignition (Figure 5c,A) turned into a larger amount of heat limited to a yellow "U" format after removal of the burner (Figure 5c,B) and in the second ignition (Figure 5c,C). This portion corresponded exactly to that of expanded material reacting to form bubbles and sparks as observed in the UL 94 test. The thickness of this "U" increases at second ignition, indicating an advance of the surficial pyrolysis zone. First, the side-edge flux of the melted material generated two points of drop detachment; after a while they turned into one point of detachment.

### 3.6. Viscosity

Viscosity plays a major role in dripping behavior. In terms of UL 94 conditions, lower viscosities ease the flow, while higher viscous forces may even prevent some melted material from separating from the polymeric source in the form of drops. The deformation and flow behavior of the polyamides under applied force was assessed by rheological measurements. The lower shear rates have been related to the dripping phenomena in polymers when they favor the viscous liquid response of these materials – a com-

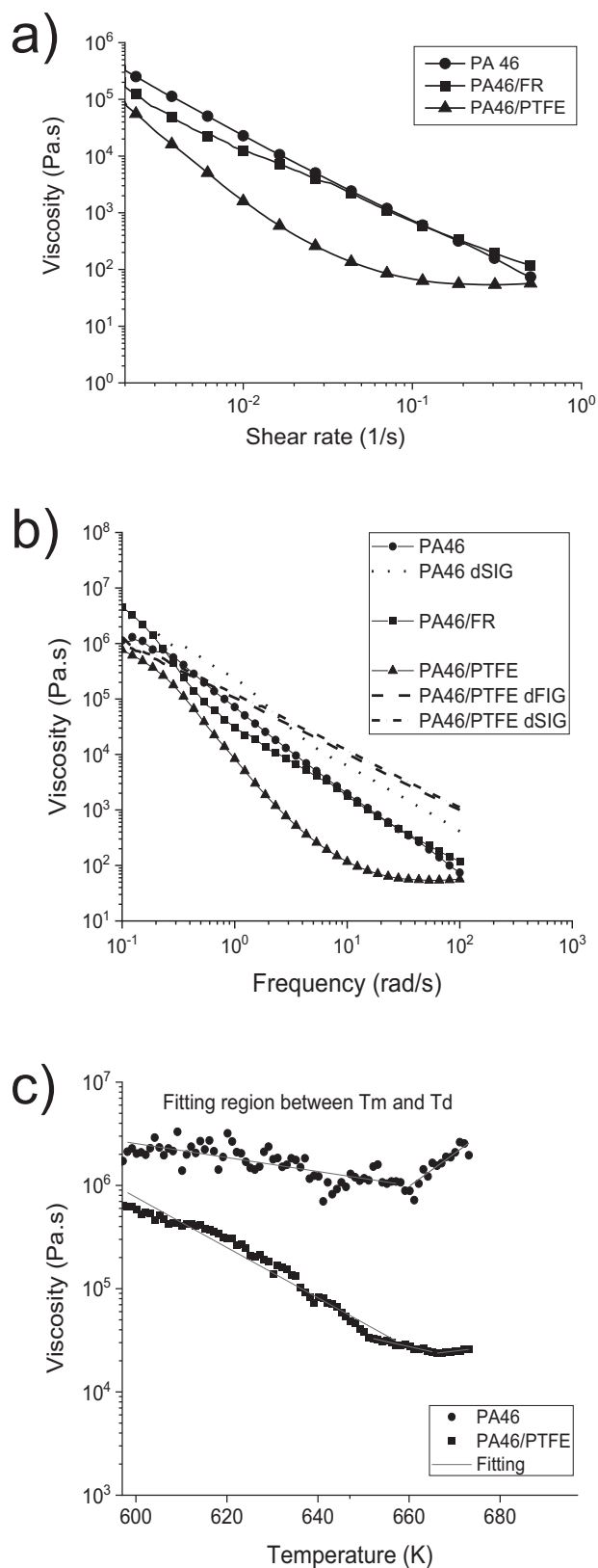
ponent of their viscoelastic state. Curves of complex viscosity (Figure 6) as a function of shear rate are shown in Figure 6a. Intermolecular hydrogen bonds and water content present in the studied polyamides tend to increase resistance towards flow at low deformation rates by acting as secondary cross-linking. This was observed in polyamide 6 materials in our previous studies. [7,12]

The viscosities of PA46 and PA46/FR were high and very similar along the range of the shear rates measured. Increasing the shear rate linearly decreases viscosity. The introduction of another polymer to the polymeric matrix (PA46/PTFE) caused a reduction in the material viscosity of one order of magnitude. This low resistance to flow can be related to a reduction in the molecular weight of the blend. It depends not only on the sum of each individual molecular weight, but also on the interaction between polymeric phases, as well as on the processing conditions and other additives that a commercial material may contain. However, the very nature of PTFE is primarily responsible for this performance once it is very sensitive to shear by its very low friction coefficient. The viscosity of the blend became independent after a shear rate of ca.  $10^{-1} \text{ s}^{-1}$ , when a plateau began to form.

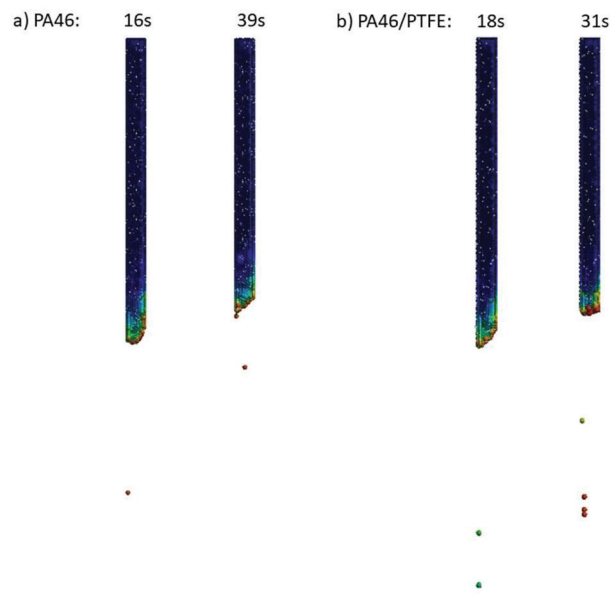
The viscosities of the drops are higher than the viscosities of the original materials (Figure 6b), due to the fact they contain an increased portion of residue which acts as reinforcement against the flow. The viscosity of dFIG from PA46 was not measured because the drops generated at first flame ignition were very few and light in weight, so that the number of drops collected was not sufficient to fill the die in order to perform rheological measurements. As to the drops from PA46/PTFE, the curves were almost superimposed, but dSIG was slightly more resistant to flow than dFIG. This result corresponds with the TGA results, which demonstrated that dSIG was more degraded than dFIG.

Figure 6c shows the curves of viscosity versus temperature for the dripping materials from 300 to 400 °C. These values were used to improve the description of viscosity in the PFEM simulations. The increase in temperature to near decomposition temperatures caused a pronounced decrease in the viscosity of the blend, while PA46 exhibited more stability. The chain uniformity and stability of one high-heat-resistant polymeric material turned out to





**Figure 6.** Complex viscosity a) versus shear rate for original materials, b) versus frequency for materials and respective drops, c) versus temperature for PA46 and PA46/PTFE.



**Figure 7.** First and last dripping was simulated by PFEM.

be more resistant to flow under high temperatures than those of two high-heat-resistant materials combined. This corresponds with the higher amount of dripping generation observed in the flammability test for PA46/PTFE than that observed for PA46. The commercial aim of this addition of PTFE to the PA46 was to produce a material with reduced friction for solid-state applications. However, PTFE also works as a dripping agent for the pyrolysis melt.

### 3.7. Numerical Results

The simulations of materials' specimens in the UL 94 vertical test were performed using PFEM. As described before, this defined problem condition configured with a total time of 40 s was applied to all materials to ensure comparability.

Images of the first and last dripping moments of each dripping material can be seen in Figure 7. PA46 and PA46/PTFE exhibited dripping behavior in the simulations (Figure 7a,b), while PA46/FR did not. The simulated results show small-size dripping behavior during the whole test, the same as was observed experimentally.

For both dripping materials, there was no dripping during the first flame application, but in the first after-flame time. Additionally, there was dripping during the second flame application and in the second after-flame time as well. These results also correspond with what was observed in the experiment. Detailed results on simulated dripping times are displayed in Figure 8 with a comparison to the experimental ones. The simulated PA46 had enhanced drop generation (Figure 8a); however, strong correspondence can be observed between the experimental and simulated dripping times, especially for PA46/PTFE (Figure 8b).

As to mass loss during the PFEM tests, the consumption of the specimens was higher than expected based on experimental results. Mass loss curves during test simulations are depicted in Figure S3 in the Supporting Information. PA46 and PA46/PTFE

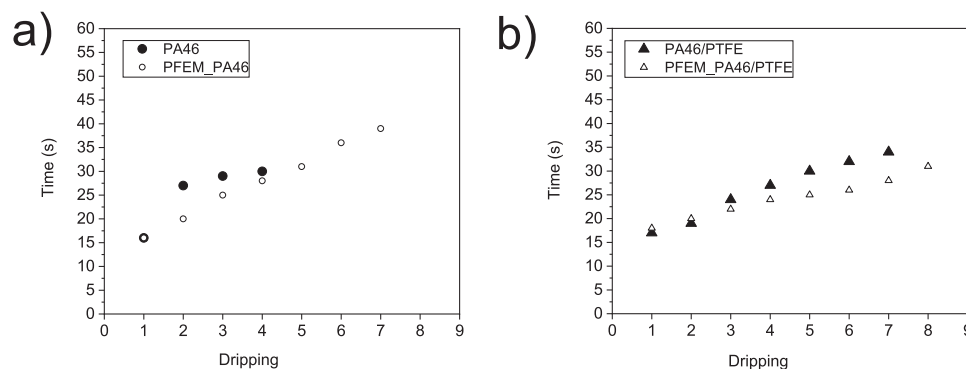


**Figure 8.** Experimental dripping time versus dripping time simulated by PFEM.

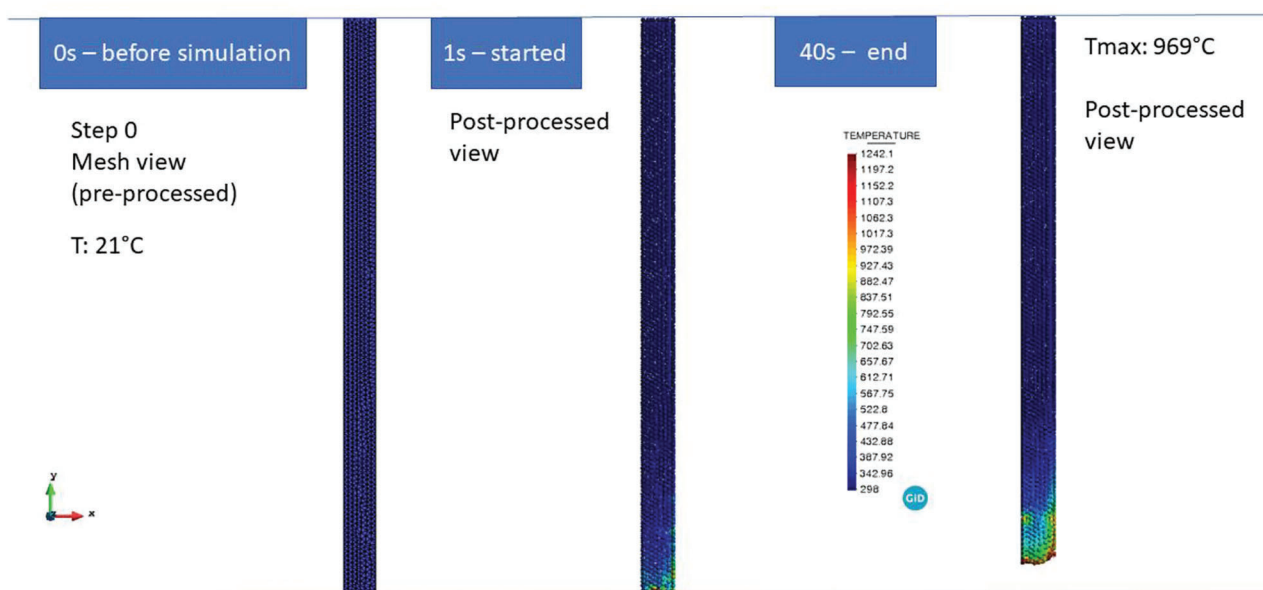


**Figure 9.** PA46/FR specimen simulated by PFEM.

presented very similar behavior. Both started to lose mass at 5 s after the first flame application (Phase I). By the end of Phase II (the first after-flame time) >2.0 wt.% was already lost. The loss in Phase III (the second flame application) was about 6.0 wt.% for both. The loss in Phase IV (the second after-flame time) was also equivalent, with PA46 exhibiting 3.7 wt.% and PA46/PTFE 4.4 wt.% mass lost. The total mass losses of PA46 and PA46/PTFE were 12.6 wt.% and 12.3 wt.%, respectively. These results deviate from that obtained experimentally (Table 2), where a significant difference was observed between these two materials, most probably due to their very different viscosities. For these materials, some properties might be of more impact than the viscosity input in the modeling. More work should be done in order to evaluate and understand this kind of response in the PFEM.

The specimen domain of PA46/FR also experienced mass loss during the test (Figure 9). As it did not drip in any test phase, the total lost portion of 4.3 wt.% was attributed to volatilization, which occurred mostly during the second flame application. This

result was a reasonable approximation of what was obtained experimentally (Table 2).

#### 4. Conclusions

High-heat-resistant polymers are commonly, and somewhat incorrectly, considered to harbor the potential for intrinsic flame retardancy. Polyamide 4.6 belongs to this polymeric class and was evaluated under UL 94 test conditions in this work. For this investigation, three commercial grades were utilized, since such high-performance materials are usually applied as they are, without any addition, mixing, or pre-processing before molding. Thus, high application specificity and special properties, which justify their elevated price are guaranteed.

However, the effects on these materials of exposure to fire was not different from that found for other less heat-resistant thermoplastics, including ignition, degradation, volatilization, charring, and flaming dripping behavior. The dripping may be considered reduced, but present. The number of drops generated by PA46

(V-1) during test was slightly decreased when compared to that observed for PA6 (V-2) in our past work.<sup>[11]</sup> However, the mass loss due to dripping for both polyamides was the same (1.4 wt.%). Clearly, the dripping behavior of the pyrolyzing melt is not a privilege of a class of polymers but depends on different phenomena. Char particles and their network structures influence the viscosity of the pyrolyzing melt, charring determines the amount of released fuel. The amount of fuel together with the effective heat of combustion but not the pyrolysis temperature controls the fire load, e.g. THR of PA46 = 24.5 kJ g<sup>-1</sup> compared to PA6 = 30.8 kJ g<sup>-1</sup> due to the high quantity of amide groups in PA46, as calculated by.<sup>[38]</sup> Melt dripping was constituted as a highly efficient cooling mechanism of the test slabs in UL<sup>94</sup>, and thus a key factor for extinguishing. Temperature profiles of the specimens showed that PA46 released their first ignition drops when decomposition temperature was achieved, and their second ignition drops when melting temperature was achieved.

The IR camera captured the increased heating activity in the specimen of PA46/FR, which did not drip. While the cooling effect in the specimen was observed for dripping materials.

Blending two high-heat-resistant polymers (PA46/PTFE) did not improve fire and dripping behavior: V-2 classification and increased dripping frequency were achieved. Thermal stability on TGA was not decreased when compared to PA46, but viscosity was drastically decreased. The low friction coefficient of PTFE affected the behavior, acting as a dripping agent. Physical deformation (expansion) of the specimen tip wrapped by charring was dominant under testing. Small-sized dripping was obtained for PA46 and PA46/PTFE experimentally and numerically. The simulated dripping times were in good agreement.

## Supporting Information

Supporting Information is available from the Wiley Online Library or from the author.

## Acknowledgements

The authors thank the National Council of Technological and Scientific Development from Brazil (CNPq) for its financial support (205385/2014-1). A.T.S.D. thanks the TU Berlin for the support with a STIBET degree completion grant.

## Conflict of Interest

The authors declare no conflict of interest.

## Data Availability Statement

The data that support the findings of this study are available from the corresponding author upon reasonable request.

## Keywords

dripping, high heat resistance, PFEM, polyamide 4.6, UL 94

Received: March 14, 2023

Revised: April 21, 2023

Published online: May 12, 2023

- [1] P. Joseph, S. Tretsiakova-Mcnally, *Materials* **2015**, *8*, 8793.
- [2] X. Wang, Y.e Song, J. Bao, *Fire Mater.* **2010**, *34*, 357.
- [3] Y. Wang, J. Jow, K. Su, J. Zhang, *J. Fire Sci.* **2012**, *30*, 477.
- [4] Y. Wang, J. Zhang, *J. Hazard. Mater.* **2013**, *246*, 103.
- [5] B. K. Kandola, D. Price, G. J. Milnes, A. Da Silva, *Polym. Degrad. Stab.* **2013**, *98*, 52.
- [6] B. K. Kandola, M. Ndiaye, D. Price, *Polym. Degrad. Stab.* **2014**, *106*, 16.
- [7] M. Matzen, B. Kandola, C. Huth, B. Schartel, *Materials* **2015**, *8*, 5621.
- [8] R. Dupretz, G. Fontaine, S. Duquesne, S. Bourbigot, *Polym. Adv. Technol.* **2015**, *26*, 865.
- [9] F. Kempel, B. Schartel, J. M. Marti, K. M. Butler, R. Rossi, S. R. Idelsohn, E. Oñate, A. Hofmann, *Fire Mater.* **2015**, *39*, 570.
- [10] Y. Wang, W. Kang, X. Zhang, C. Chen, P. Sun, F. Zhang, S. Li, *Fire Mater.* **2018**, *42*, 436.
- [11] A. Turski Silva Diniz, C. Huth, B. Schartel, *Polym. Degrad. Stab.* **2020**, *171*, 109048.
- [12] C. Hu, G. Fontaine, P. Tranchard, T. Delaunay, M. Collinet, S. Marcille, S. Bourbigot, *Polym. Degrad. Stab.* **2018**, *155*, 145.
- [13] Y. Yu, L. Xi, M. Yao, L. Liu, Y. Zhang, S. Huo, Z. Fang, P. Song, *iScience* **2022**, *25*, 103950.
- [14] D. G. J. Seah, A. Dasari, *Polym. Test.* **2023**, *118*, 107893.
- [15] DSM, Stanyl Brochure, www.dsm.com, accessed: April, 2020.
- [16] IEC 60695-11-10: Test flames - 50 W horizontal and vertical test flame methods. International Electrotechnical Commission. 2013.
- [17] E. Oñate, S. R. Idelsohn, F. Del Pin, R. Aubry, *Int. J. Numer Methods Eng.* **2004**, *1*, 267.
- [18] M. Cremonesi, A. Franci, S. Idelsohn, E. Oñate, *Arch. Comput. Methods Eng.* **2020**, *27*, 1709.
- [19] E. Oñate, R. Rossi, S. R. Idelsohn, K. M. Butler, *Int. J. Numer Methods Eng.* **2010**, *81*, 1046.
- [20] J. Marti, B. Schartel, E. Oñate, *J. Fire Sci* **2022**, *40*, 3.
- [21] J. Marti, S. R. Idelsohn, E. Oñate, *Fire Technol.* **2018**, *54*, 1783.
- [22] M. Matzen, J. Marti, E. E. Oñate, S. R. Idelsohn, B. Schartel, in *Conference Proceedings Fire and Materials*, International conference 15th, **2017**, 57.
- [23] S. I. Stoliarov, N. Safronava, R. E. Lyon, *Fire Mater.* **2009**, *33*, 257.
- [24] S. V. Levchik, E. D. Weil, M. Lewin, *Polym. Int.* **1999**, *48*, 532.
- [25] J. Pagacz, A. Leszczynska, M. Modesti, C. Boaretti, M. Roso, I. Malka, K. Pielichowski, *Thermochim. Act.* **2015**, *612*, 40.
- [26] S. I. Stoliarov, R. N. Walters, *Polym. Degrad. Stab.* **2008**, *93*, 422.
- [27] A. Hamins, *J. Fire Protect. Eng.* **2005**, *15*, 265.
- [28] T. Nyazika, M. Jimenez, F. Samyn, S. Bourbigot, *J. Fire Sci.* **2019**, *37*, 377.
- [29] F. Kempel, B. Schartel, G. T. Linteris, S. I. Stoliarov, R. E. Lyon, R. N. Walters, A. Hofmann, *Combust. Flame* **2012**, *159*, 2974.
- [30] S. K. Mukhopadhyay, in *Handbook of Tensile Properties of Textile and Technical Fibres*, Woodhead Publishing, Oxford **2009**, pp. 197–222.
- [31] J. E. Mark, *Polymer Data Handbook*, Oxford University Press Inc., New York **1999**.
- [32] (Eds: P. J. DiNenno), *SFPE Handbook of Fire Protection Engineering*, 3rd ed., National Fire Protection Association. Quincy, MA **2002**.
- [33] S. V. Levchik, E. D. Weil, *Polym. Int.* **2000**, *49*, 1033.
- [34] K. H. Pawlowski, B. Schartel, *Polym. Int.* **2007**, *56*, 1404.
- [35] A. B. Morgan, C. A. Wilkie, *Flame Retardant Polymer Nanocomposites*, Wiley, Hoboken, NJ. **2007**.
- [36] E. D. Weil, S. V. Levchik, *Flame Retardants for Plastics and Textiles: Practical Applications*, Hanser, Munich, Germany **2016**.
- [37] Applied Plastics Technology, Inc., Teflon™ PTFE, www.ptfeparts.com accessed: November, **2022**.
- [38] R. Sonnier, B. Otazaghine, F. Iftene, C. Negrell, G. David, B. A. Howell, *Polymer* **2016**, *86*, 42.